Journal of Insect Science, (2018) 18(3): 23; 1–10
doi: 10.1093/jisesa/iey064
Research

Multiple Glutathione S-Transferase Genes in *Heortia vitessoides* (Lepidoptera: Crambidae): Identification and Expression Patterns

Jie Cheng,[1] Chun-Yan Wang,[1] Zi-Hao Lyu,[1] and Tong Lin[1,2]

[1]College of Forestry and Landscape Architecture, South China Agricultural University, Wushan Street, Guangzhou, Guangdong 510642, China and [2]Corresponding author, e-mail: lintong@scau.edu.cn

Subject Editor: Yu-Cheng Zhu

Received 20 April 2018; Editorial decision 30 May 2018

Abstract

To elucidate the role of glutathione S-transferases (GSTs) in *Heortia vitessoides* Moore (Lepidoptera: Crambidae), one of the most destructive defoliating pests in *Aquilaria sinensis* (Lour.) Gilg (Thymelaeaceae) forests, 16 GST cDNAs were identified in the transcriptome of adult *H. vitessoides*. All cDNAs included a complete open reading frame and were designated *HvGSTd1–HvGSTu2*. A phylogenetic analysis showed that the 16 *HvGSTs* were classified into seven different cytosolic classes; three in delta, two in epsilon, three in omega, three in sigma, one in theta, two in zeta, and two in unclassified. The expression patterns of these *HvGSTs* in various larval and adult tissues, following exposure to half the lethal concentrations (LC_{50}s) of chlorantraniliprole and beta-cypermethrin, were determined using real-time quantitative polymerase chain reaction (RT-qPCR). The expression levels of the 16 *HvGSTs* were found to differ among various larval and adult tissues. Furthermore, the RT-qPCR confirmed that the transcription levels of nine (*HvGSTd1*, *HvGSTd3*, *HvGSTe2*, *HvGSTe3*, *HvGSTo3*, *HvGSTs1*, *HvGSTs3*, *HvGSTu1*, and *HvGSTu2*) and six (*HvGSTd1*, *HvGSTd3*, *HvGSTe2*, *HvGSTo2*, *HvGSTs1*, and *HvGSTu1*) *HvGST* genes were significantly higher in the fourth-instar larvae following exposure to the insecticides chlorantraniliprole and beta-cypermethrin, respectively. These genes are potential candidates involved in the detoxification of these two insecticides. Further studies utilizing the RNA interference approach are required to enhance our understanding of the functions of these genes in this forest pest.

Key words: glutathione S-transferase, expression pattern, insecticide treatment

The glutathione S-transferases (GSTs, EC 2.5.1.18) comprise a diverse family of enzymes found ubiquitously in aerobic organisms (Enayati et al. 2005). They catalyze the conjugation of electrophilic substrates to glutathione (GSH), enabling the organisms to metabolize a wide range of endogenous and exogenous compounds (Huang et al. 2017). Some GSTs can serve as Se-independent GSH peroxidases, maleylacetoacetate isomerases, and thiol transferases, and perform noncatalytic binding functions (Yu et al. 2008, Zhang et al. 2014). Moreover, insect GSTs play an important role in ecdysteroid biosynthesis, larval development, immune response, and odorant inactivation (Rogers et al. 1999, Huang et al. 2011, Enya et al. 2015). Two domains in GSTs are responsible for their detoxification function: the GSH-binding site (G-site) located in the N-terminal domain and the hydrophobic substrate-binding pocket (H-site) in the C-terminal domain (Enayati et al. 2005). Based on their cellular locations, GSTs are divided into three different classes—cytosolic, microsomal, and mitochondrial. However, mitochondrial GSTs have not yet been found in insects (Han et al. 2016). The insect cytosolic GSTs were assigned to seven distinct classes—delta, epsilon, omega, sigma, theta, zeta, and unclassified—according to their sequence identities, substrate specificities, and immunological properties (Sheehan et al. 2001, Yu et al. 2008). Among the cytosolic GSTs, delta and epsilon were the only insect-specific classes, and the other five classes were present in mollusks, nematodes, and mammals (Labade et al. 2018).

Owing to the vital role of GSTs in xenobiotic detoxification, research on insect GSTs has historically been focused on their role in insecticide resistance (Feng et al. 1999). Increased GST activity has been reported to be one of the main reasons for insecticide resistance in other lepidopteran species, such as *Helicoverpa armigera* Hübner (Labade et al. 2018), *Spodoptera exigua* Hübner (Wan et al. 2016), and *Bombyx mori* Linnaeus (Yamamoto and Yamada 2016). *Heortia vitessoides* Moore (Lepidoptera: Crambidae) is a serious defoliating pest of *Aquilaria sinensis* (Lour.) Gilg (Thymelaeaceae) Sprenger that produces valuable agarwood, a fragrant wood widely used in the traditional medicine and incense industries (Jin et al. 2016, Cheng et al.

2017). The distribution of *H. vitessoides* ranges from India, Nepal, China, Sri Lanka, through South-East Asia and the East Indies to Queensland, the New Hebrides, and Fiji (Kalita et al. 2002, Qiao et al. 2013). This insect has seven or eight generations per year in southern China, and completely consumes the leaves of *A. sinensis*, causing severe economic losses. In past decades, the management of *H. vitessoides* has relied on the spraying of conventional insecticides, such as chlorantraniliprole and beta-cypermethrin. However, these insecticides, and even their mixtures, have become less efficient at controlling this serious pest (Su 1994, Chen et al. 2011, Qiao et al. 2012). Therefore, it was necessary to investigate whether GSTs in *H. vitessoides* contribute to the detoxification of these two insecticides.

In the present study, we identified 16 full-length cytosolic GST sequences in *H. vitessoides*. The transcription profiles of these 16 genes in different larval and adult tissues were investigated by real-time quantitative polymerase chain reaction (RT-qPCR). Furthermore, their responses to chlorantraniliprole and beta-cypermethrin were also investigated by determining their expression levels. To our knowledge, this is the first report on the identification and characterization of multiple GST genes in this forest pest.

Materials and Methods

Insects

The *H. vitessoides* larvae and adults were originally collected from an *A. sinensis* plantation in Tianlu Lake Forest Park (23°15′N, 113°25′E) of Guangzhou, Guangdong, China. All insects were reared in the laboratory, which was maintained at a temperature of 26°C and a relative humidity of 70 ± 2% with a photoperiod of 14:10 (L:D) h. Insects were anesthetized on ice and dissected into different tissues (midgut, Malpighian tubules, and fat body of the 2-d-old fourth-instar larvae; and antenna, abdomen, and leg of the 3-d-old adults). All tissue samples were immediately frozen in liquid nitrogen and stored at −80°C.

Insecticide Treatment

The insecticides chlorantraniliprole and beta-cypermethrin were purchased from Fengle Agrochemical Co., Ltd. (Hefei, China) and diluted with analytical-grade acetone to make a working solution of 7.7×10^{-4} mg/liter for chlorantraniliprole and 8.9×10^{-5} mg/liter for beta-cypermethrin (LC_{50} values) (Chen et al. 2011). The freshly molted (<24 h) fourth-instar larvae were selected and starved for 2 h. The leaf-dipping method was employed to investigate the insecticidal activity (Chen and Zhang 2015). Fresh *A. sinensis* leaves were dipped into the pesticide solutions for 10–15 s, air-dried at 26°C, and then fed to the starved larvae. The control insects were fed with the *A. sinensis* leaves treated only with acetone. The insecticide-treated and control insects were collected after 24 h, immediately frozen in liquid nitrogen, and stored at −80°C prior to RNA extraction. Each sample consisted of 15 larvae with three independent replicates.

Homology Search and Sequence Verification

The GST transcripts were retrieved from the transcriptome of adult *H. vitessoides* (accession number: SRX3035102; Cheng et al. 2017) by keyword searching. The sequences of GSTs were confirmed by comparing them with the other sequences available in the National Center for Biotechnology Information (NCBI) GenBank using the nucleotide BLAST and BLAST-X tools. To confirm the above result, the corresponding pair of GST-specific primers (Table 1) was designed with Primer Premier 5.0 (Premier Biosoft International, Palo Alto, CA) to clone the complete or partial open reading frames (ORFs). The PCR product was gel-purified, ligated into the pClone007 simple vector (TSINGKE Bio, Guangzhou, China), transformed into *Escherichia coli* DH5α competent cells (Takara Bio, Otsu, Japan), and sequenced (TSINGKE Bio, Guangzhou, China). The identities of the recovered cDNAs of *H. vitessoides* were confirmed using BLASTx analyses.

Bioinformatic Analyses

The GST-ORFs were identified using ORF Finder software (http://www.ncbi.nlm.nih.gov/gorf/gorf.html). The conserved sites were predicted by searching the Conserved Domain Database (http://https://www.ncbi.nlm.nih.gov/Structure/cdd/wrpsb.cgi). The Compute pI/Mw tool, available in the ExPASy server (http://web.expasy.org/compute_pi/), was used to predict the isoelectric points (pI) and molecular weights (MW) of the predicted proteins. The homologous protein sequences from various species were obtained from the NCBI database, and the GenBank accession numbers of the sequences used are listed in Supp Table 1 [online only]. The amino acid sequences of the GST proteins were aligned in Clustal Omega (http://www.ebi.ac.uk/Tools/msa/clustalo/). A phylogenetic tree was constructed using the neighbor-joining (NJ) method in MEGA 5.0 software (Tamura et al. 2011). The node support was assessed using a bootstrap procedure based on 1,000 replicates.

RNA Extraction and cDNA Synthesis

Total RNA was isolated from different tissues of *H. vitessoides* larvae and adults, as well as from the tissues of insecticide-treated and control larvae, using the E.Z.N.A. Total RNA Kit II (OMEGA Biotec, Norcross, GA) according to the manufacturer's instructions. The quality of the RNA of each individual sample was visualized on denaturing agarose gel, and the RNA concentrations were estimated using Nanodrop 2000 (NanoDrop Products, Wilmington, DE). The first-strand cDNA samples were synthesized from 2 μg of the total RNA using the PrimeScript RT Reagent Kit with gDNA Eraser (Takara Bio, Otsu, Japan), and then immediately stored at −80°C for further use.

Real-Time Quantitative PCR

An RT-qPCR was performed using SYBR Premix Ex Taq II (Takara Bio, Otsu, Japan). Each reaction (20 μl volume) contained 2 μl of cDNA, 10 μl of SYBR Premix Ex Taq, 0.4 μl of forward and reverse primers (10 μM), and 7.2 μl of RNase-free double-distilled water. The gene-specific primers (Table 1) were designed using Primer Premier 5.0 (Premier Biosoft International, Palo Alto, CA). Two reference genes, *α-tubulin* (GenBank MG132200) and *β-actin* (GenBank MG132199), were used as internal controls for RT-qPCR to normalize target gene expression (Cheng et al. 2018). The RT-qPCR was carried out in 96-well plates using a LightCycler (Roche Diagnostics, Indianapolis, IN). The amplification conditions were as follows: initial denaturation at 95°C for 5 min; 40 cycles at 95°C for 10 s, 60°C for 20 s; and cooling at 40°C for 30 s. The nontemplate reactions (replacing cDNA with diethyl pyrocarbonate water) were used as negative controls, and the results were analyzed by the LightCycler Real-Time PCR System. Three biological replicates and three technical replicates were used for the RT-qPCR analysis. The quantity of GST mRNAs was calculated using the $2^{-\Delta\Delta Ct}$ method (Pfaffl 2001).

Statistical Analysis

The gene expression data are presented as the means ± SD for three independent replicates. A one-way analysis of variance (ANOVA; Systat, Inc., Evanston, IL), followed by Tukey's test ($P < 0.05$), was

Table 1. Primers used in this study

Gene	Direction	Sequence (5′→3′)	Product size (bp)	PCR type
HvGSTd1	F	TGGCAAACAGAACACAGG	353	RT-qPCR
	R	CAGGCATCTTGCTGTTCTT		
HvGSTd2	F	ACCAGTTTCGGTGCGTCT	242	RT-qPCR
	R	TACTGTGTGCTGGGGGTT		
HvGSTd3	F	CCACAGCATACAGTCCCT	335	RT-qPCR
	R	CACTAACGCCAAGTCTGC		
HvGSTe2	F	CTACCAGCAGGAGAACAT	152	RT-qPCR
	R	GTAGAGGCTGTCGTTTTG		
HvGSTe3	F	CAAAGGACCATCTCAAGG	273	RT-qPCR
	R	TCTGGCGTGTAGGACTTT		
HvGSTo1	F	ATTTCCACAAGGGGCTCG	280	RT-qPCR
	R	TCCCTTAGCCCGAGATTCC		
HvGSTo2	F	GGTGATGCGTTACCTCCA	301	RT-qPCR
	R	TTGTCCTGGGCTTTCTGC		
HvGSTo3	F	ACCGAGTGCTCCTCATCCT	224	RT-qPCR
	R	AGGGGTCGTTTGCGTGTA		
HvGSTs1	F	ATGGCGGTCAGGACTTTG	225	RT-qPCR
	R	CGGATGTCGTTGAGGAAG		
HvGSTs2	F	CTGTGTTGGATGCTGCGGT	207	RT-qPCR
	R	AGGATGAAGTCAGCCCAGG		
HvGSTs3	F	GATGCCTTACCATTCGGG	334	RT-qPCR
	R	AGGACAAAGTCAGCCCAG		
HvGSTt1	F	GACAAATCCAGGAAGCAG	141	RT-qPCR
	R	ACAAGTCAGCCACAGTCA		
HvGSTz1	F	ACAAGACCACAAAGACCC	215	RT-qPCR
	R	GTATTTCCCAGCACAAGC		
HvGSTz2	F	TATCATCGTGCTCCTGGC	158	RT-qPCR
	R	CGCCATCAATAACCAGGG		
HvGSTu1	F	CGAAGAGGTTGTCCCGTT	234	RT-qPCR
	R	AAGCCGTCGTCATCCAAC		
HvGSTu2	F	TCCATCGGTGTTCCTGTA	142	RT-qPCR
	R	ATAGCACGACTTTCCCAC		
β-actin	F	GTGTTCCCCTCTATCGTGG	119	RT-qPCR
	R	TGTCGTCCCAGTTGGTGAT		
α-tubulin	F	GATGCCCACAGACAAGACC	437	RT-qPCR
	R	AGTGTGGGTGGTCAGGATG		
HvGSTd1	F	ATTCAATCCGCTGATAGGTG	741	ORF
	R	CATCAATGTCGTCATAGCCA		
HvGSTd2	F	TAGAACAATGCCTTTGGACC	597	ORF
	R	CTCTTCGTATCCAGGTGC		
HvGSTd3	F	TGTCGTTTAGTGCTGCTG	602	ORF
	R	AGCCTTCAGTTGAGCCAC		
HvGSTe2	F	ATACAAAAAGGATACCAGCCCC	642	ORF
	R	TTCACCCGCCAACCACTT		
HvGSTe3	F	TGTTCACAAAGGACCATCTC	392	ORF
	R	TGATAGAAGACAGGCAGC		
HvGSTo1	F	TTCTGCCTCCATACAACG	659	ORF
	R	TAGCCCGAGATTCCGTAA		
HvGSTo2	F	GGTGATGCGTTACCTCCA	473	ORF
	R	ATAACCAGGCACATCTCC		
HvGSTo3	F	ACCGAGTGCTCCTCATCCT	518	ORF
	R	CTCCCCAATCCGCAAAGT		
HvGSTs1	F	TGTTACTGTCCTATGGCG	481	ORF
	R	CTTGAATGCGGGGAACTT		
HvGSTs2	F	AGATACATTCTCCACTACGC	452	ORF
	R	GTCAAAGAAAAGGTTCGCTG		
HvGSTs3	F	GCTGAGCCGATAAGATAC	466	ORF
	R	TGTCCGAGGGATAAGTTG		
HvGSTt1	F	ACCTTATGTCCCAGCCTT	491	ORF
	R	CAAACAAGTCAGCCACAGT		
HvGSTz1	F	CAGAGAGGTGAACCCCAT	400	ORF
	R	GGAATGGTCGCAGGTCTA		
HvGSTz2	F	ACGGCTTCAAGTTATCATCG	382	ORF
	R	GTCGCACCAGTATTTTGAG		
HvGSTu1	F	GAAGAGGTTGTCCCGTTA	532	ORF
	R	GGAAGTCAGCAATGGTCA		
HvGSTu2	F	CGACGGTTTTATTGTGTGG	752	ORF
	R	GGTAGAGAAGTGACAGATAGAC		

Table 2. Details of the 16 GSTs identified in *Heortia vitessoides*

Group	Gene name	Accession number	ORF (bp/aa)	Predicted MW (kDa)	Theoretical pI	Top BLASTx hit		
						Species	*E*-value	%ID	Accession number
Delta	*HvGSTd1*	MG879004	810/269	30.78	6.53	*Cnaphalocrocis medinalis*	8e-143	76	AIL29308.1
	HvGSTd2	MG879005	651/216	24.63	6.53	*Chilo suppressalis*	2e-100	79	AKS40339.1
	HvGSTd3	MG879006	657 /218	24.16	4.69	*Ostrinia furnacalis*	1e-97	72	AEF98444.1
Epsilon	*HvGSTe2*	MG879008	672/223	25.66	6.22	*Chilo suppressalis*	9e-126	75	AKS40343.1
	HvGSTe3	MG879007	651/216	24.79	5.02	*Cnaphalocrocis medinalis*	8e-113	68	AIL29312.1
Omega	*HvGSTo1*	MG879010	765/254	28.81	5.90	*Chilo suppressalis*	1e-169	89	AKS40345.1
	HvGSTo2	MG879011	813/270	31.27	7.61	*Chilo suppressalis*	4e-138	70	AKS40346.1
	HvGSTo3	MG879012	723/240	28.58	6.24	*Cnaphalocrocis medinalis*	1e-160	88	AIZ46903.1
Sigma	*HvGSTs1*	MF521977	615/204	23.20	5.24	*Chilo suppressalis*	3e-114	76	AMY26653.1
	HvGSTs2	MG879009	612/203	23.40	8.73	*Chilo suppressalis*	5e-102	72	AKS40349.1
	HvGSTs3	MG879018	615/204	23.74	8.84	*Ostrinia furnacalis*	8e-103	70	AAF23078.1
Theta	*HvGSTt1*	MG879013	687/228	26.58	8.69	*Bombyx mori*	1e-109	68	NP_001108463.1
Zeta	*HvGSTz1*	MG879014	687/228	25.16	6.39	*Cydia pomonella*	1e-149	96	ARM39005.1
	HvGSTz2	MG879015	648/215	24.64	9.10	*Cnaphalocrocis medinalis*	7e-103	67	AIL29322.1
Unclassified	*HvGSTu1*	MG879016	702/233	26.70	6.24	*Chilo suppressalis*	1e-147	84	AKS40352.1
	HvGSTu2	MG879017	648/215	24.17	5.68	*Cnaphalocrocis medinalis*	4e-126	84	AIL29324.1

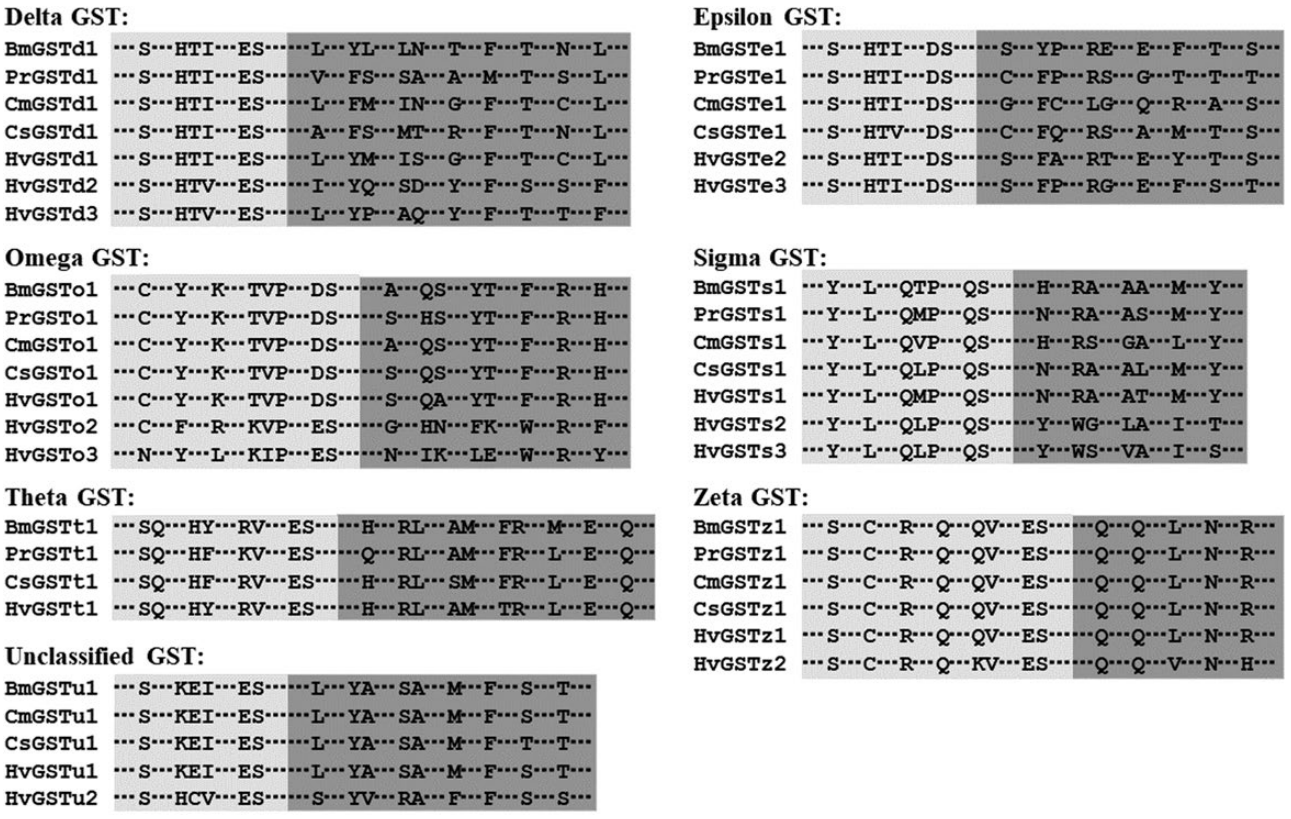

Fig. 1. Sequence alignment of the conserved GST sites from *Bombyx mori* (Bm), *Pieris rapae* (Pr), *Cnaphalocrocis medinalis* (Cm), *Chilo suppressalis* (Cs), and *Heortia vitessoides* (Hv). The amino acid residues not shown here are represented by three sequential dots. The predicted GSH-binding sites (G-sites) are shaded in light gray and the substrate-binding pockets (H-sites) are shaded in dark gray. The GenBank accession numbers are shown in Supp Table 1 [online only].

performed to compare the differences among different tissues. To compare the differences in gene expression between the insecticide-treated and control larvae, a paired Student's *t*-test was performed. Differences were considered statistically significant at $P < 0.05$. The data analysis was conducted using SPSS 18.0 (SPSS, Inc., Chicago, IL).

Results

Identification and Characterization of GST Genes From *H. vitessoides*

In total, 16 cDNA sequences encoding putative GSTs were identified in the *H. vitessoides* transcriptome data, and designated as *HvGSTd1–HvGSTu2* (Table 2). All *HvGST* cDNAs included a complete ORF. The sizes of the deduced *HvGST* proteins ranged from 203 to 270 amino acid residues, and their predicted protein MW ranged from 23.20 to 31.27 kDa, with theoretical pI values of 4.69–9.10 (Table 2). The amino acid sequence identities were 42.7–58.6% among the three delta GSTs, 58.8% between the two epsilon GSTs, 28.6–40.2% among the three omega GSTs, 32.3–64.5% among the three sigma GSTs, 40.2% between the two zeta GSTs, and 28.9% between the two unclassified GSTs (Supp Table 2 [online only]). These *HvGST* genes have been deposited in GenBank, and their accession numbers are given in Table 2.

The details of the BLASTX search of the best hits for all 16 *HvGST* genes are shown in Table 2. All *HvGST* genes had a relatively

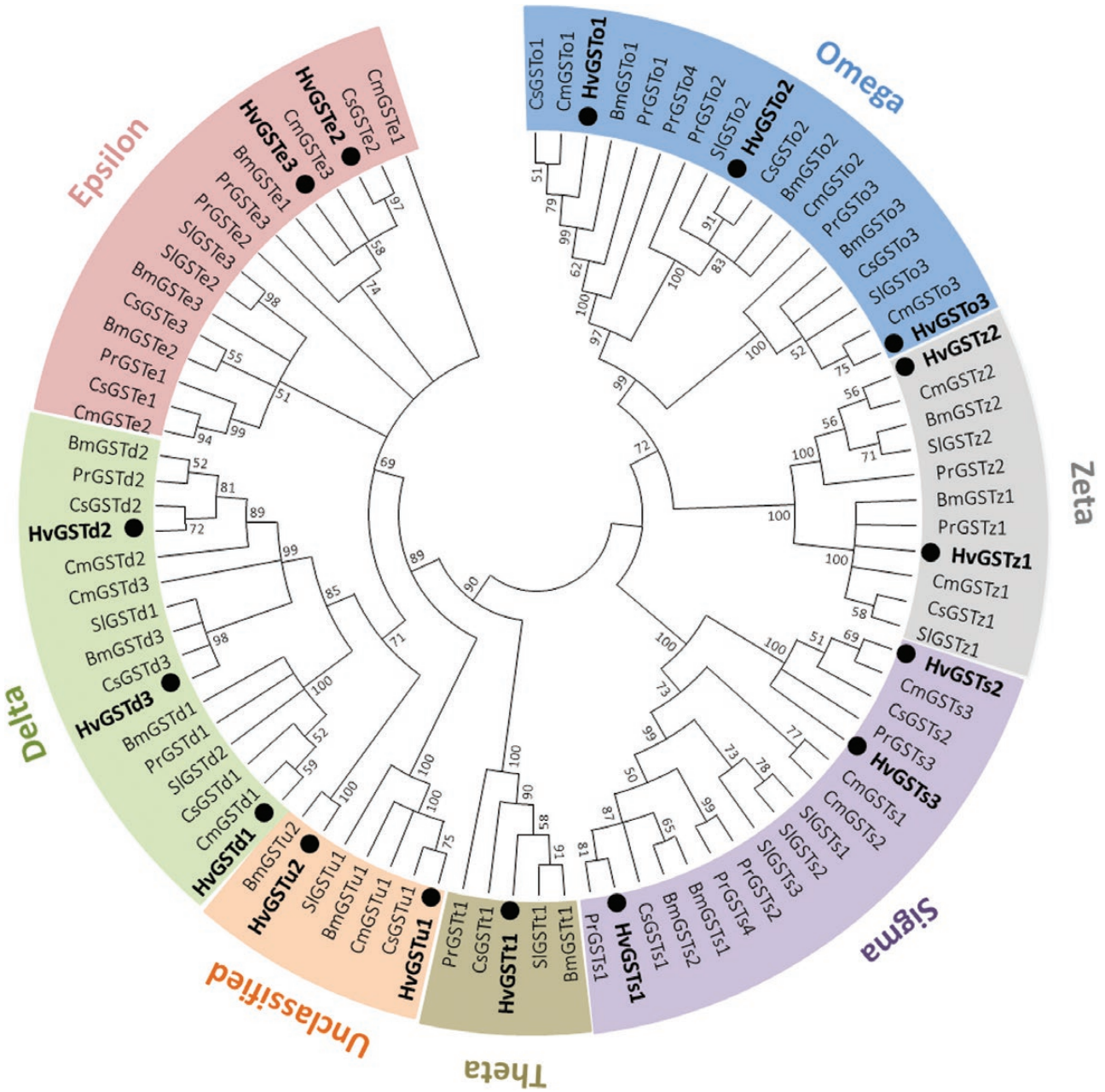

Fig. 2. Phylogenetic analysis of GSTs from *Pieris rapae* (Pr), *Bombyx mori* (Bm), *Cnaphalocrocis medinalis* (Cm), *Chilo suppressalis* (Cs), *Spodoptera litura* (Sl), and *Heortia vitessoides* (Hv). Insect GSTs are classified into seven distinct classes (delta, epsilon, omega, sigma, theta, zeta, and unclassified). The 16 *H. vitessoides* GSTs (*HvGSTs*) are highlighted with black circles. The GenBank accession numbers and amino acid sequences used for phylogenetic tree construction are given in Supp Table 1 [online only].

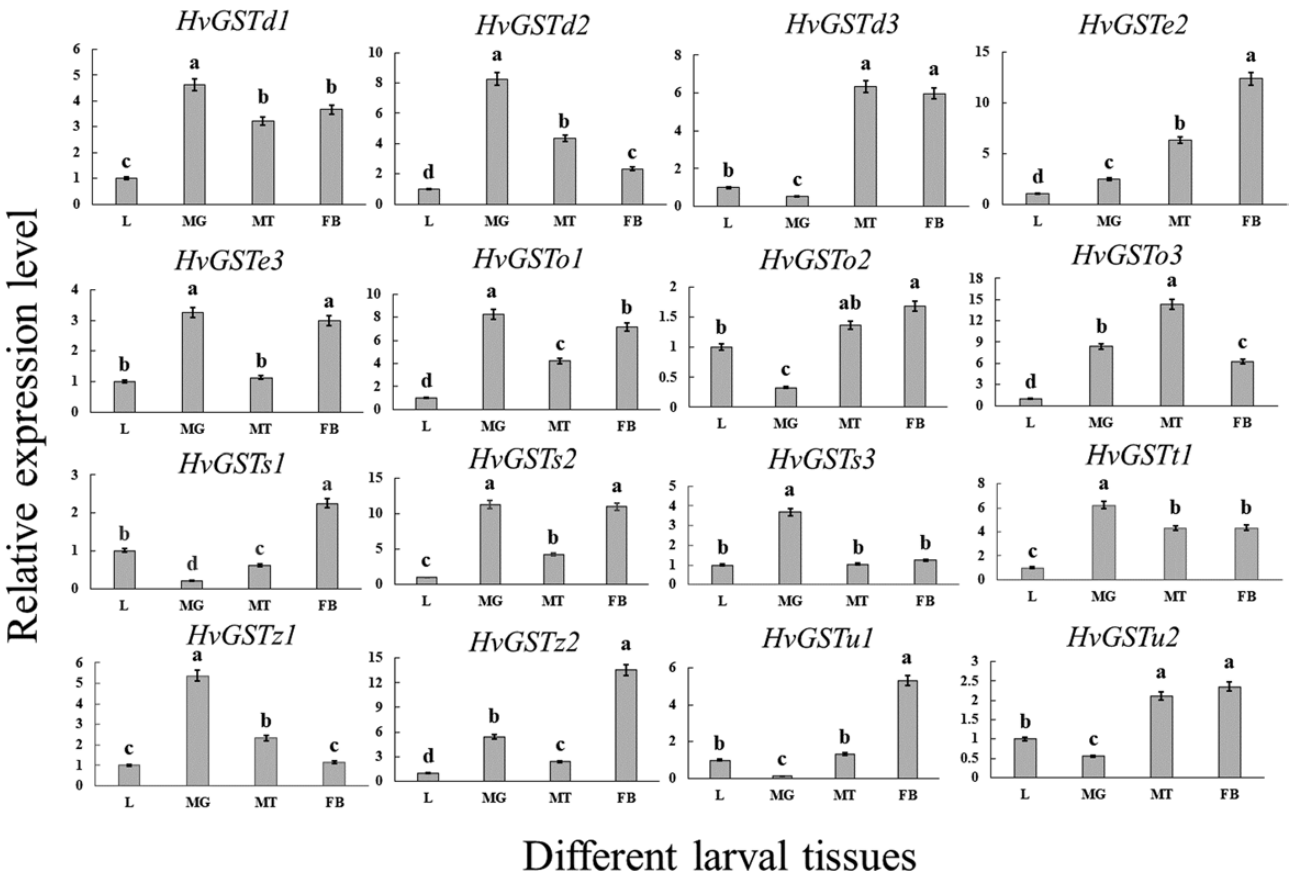

Fig. 3. Relative expression levels of 16 *HvGST* genes in various larval tissues. L (2-d-old fourth-instar larvae), MG (midgut), MT (Malpighian tubules), and FB (fat body). The *HvGST* expression levels in different larval tissues were normalized relative to those in the 2-d-old fourth-instar larvae. Different letters indicate significant differences at $P < 0.05$ according to one-way analysis of variance (ANOVA), followed by Tukey's test. The data represent the mean ± SD of three biological replicates.

high sequence identity (67–96%), with their respective orthologs from other lepidopteran species. A multiple sequence alignment revealed that a G-site in the N-terminal domain and an H-site in the C-terminal domain are present in all of the deduced *H. vitessoides* GST proteins (Fig. 1).

A phylogenetic analysis was conducted to evaluate the relationships between the *HvGSTs* and GSTs from five other lepidopteran species. In the phylogenetic tree (Fig. 2), the 16 *HvGSTs* were allocated to seven groups representing different GST classes, including three in delta (*HvGSTd1*, *HvGSTd2*, and *HvGSTd3*), two in epsilon (*HvGSTe2* and *HvGSTe3*), three in omega (*HvGSTo1*, *HvGSTo2*, and *HvGSTo3*), three in sigma (*HvGSTs1*, *HvGSTs2*, and *HvGSTs3*), one in theta (*HvGSTt1*), two in zeta (*HvGSTz1* and *HvGSTz1*), and two in unclassified (*HvGSTu1* and *HvGSTu2*). Each *HvGST* gene clustered with at least one orthologous protein from the other lepidopteran species (Fig. 2).

Expression of *HvGSTs* in Different Larval and Adult Tissues

To determine the expression levels of 16 *HvGST* genes in different tissues of the larvae and adults of *H. vitessoides*, the cDNAs obtained from different tissues were used as the templates for RT-qPCR. The expression levels of the 16 *HvGST* genes were different in various larval tissues. Most *HvGST* genes (*HvGSTd1*, *HvGSTd2*, *HvGSTe2*, *HvGSTo1*, *HvGSTo3*, *HvGSTs2*, *HvGSTt1*, and *HvGSTz2*) were ubiquitously expressed in all tested tissues (Fig. 3). Other *HvGST* genes, such as *HvGSTd3* and *HvGSTu2*, were expressed predominately in the Malpighian tubules and fat body while *HvGSTz1* and *HvGSTs3* were abundantly expressed in the midgut (Fig. 3).

The expression patterns of 16 *HvGST* genes in three different adult tissues revealed relatively high mRNA expression levels of most *HvGST* genes (*HvGSTd2*, *HvGSTd3*, *HvGSTe2*, *HvGSTe3*, *HvGSTo1*, *HvGSTo3*, *HvGSTs1*, *HvGSTs3*, *HvGSTt1*, *HvGSTz1*, *HvGSTz2*, *HvGSTu1*, and *HvGSTu2*) in the abdomen (Fig. 4). Two *HvGST* genes were mainly expressed in two adult tissues—*HvGSTd1* in the abdomen and antenna and *HvGSTs2* in the abdomen and leg (Fig. 4).

Expression of *HvGSTs* in the Larvae Exposed to Insecticides

The transcriptional changes of the 16 *HvGST* genes in the fourth-instar larvae after an exposure to LC_{50}s of chlorantraniliprole and beta-cypermethrin were determined by RT-qPCR. In the chlorantraniliprole-treated insects, the expression of nine *HvGST* genes (*HvGSTd1*, *HvGSTd3*, *HvGSTe2*, *HvGSTe3*, *HvGSTo3*, *HvGSTs1*, *HvGSTs3*, *HvGSTu1*, and *HvGSTu2*) was significantly higher than in the control insects after 24 h of chlorantraniliprole exposure, and the expression of three *HvGST* genes (*HvGSTs2*, *HvGSTz1*, and *HvGSTz2*) was markedly downregulated with respect to those in the control insects (Fig. 5). In the beta-cypermethrin-treated insects, the expression of six *HvGST* genes (*HvGSTd1*, *HvGSTd3*, *HvGSTe2*, *HvGSTo2*, *HvGSTs1*, and *HvGSTu1*) was significantly upregulated with respect to the control

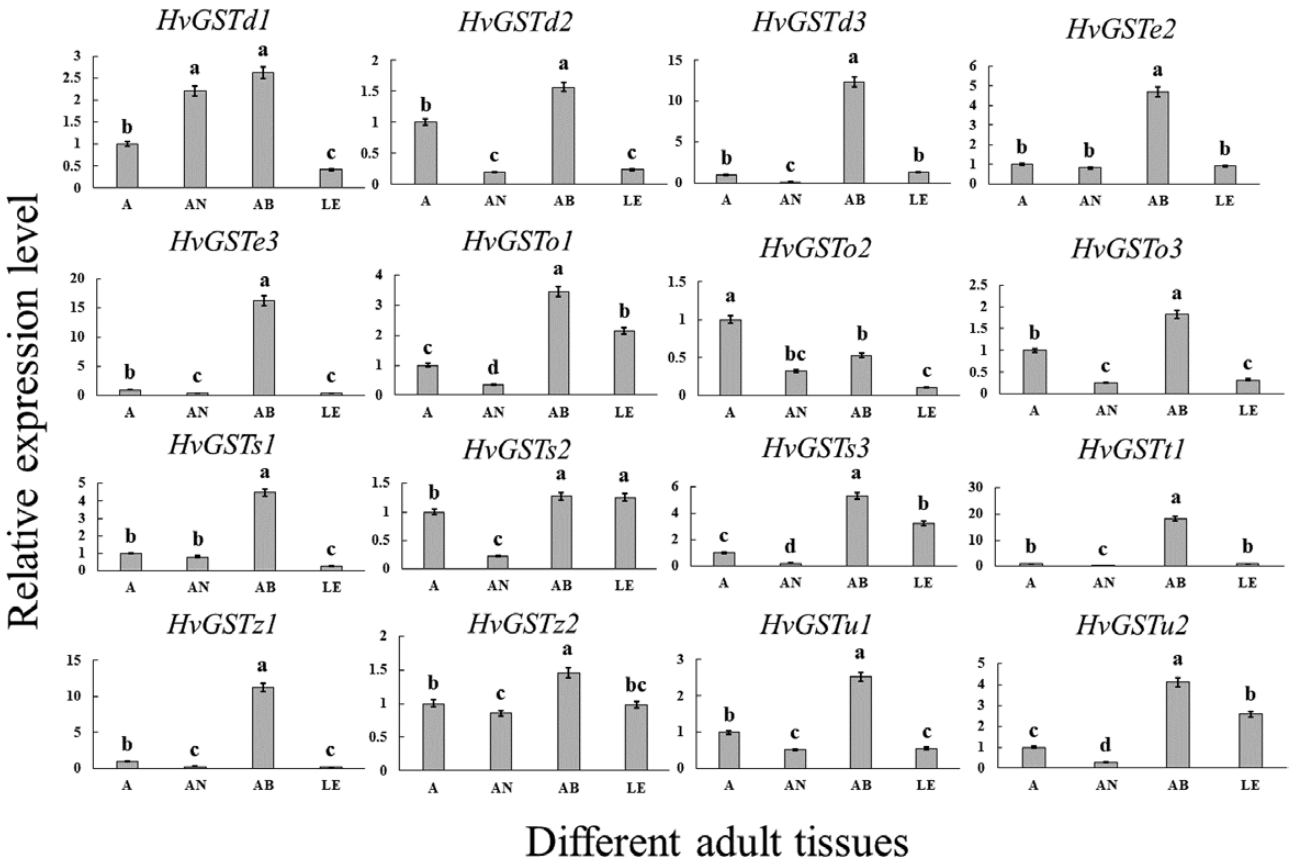

Fig. 4. Relative expression levels of 16 *HvGST* genes in various adult tissues. A (3-d-old adults), AN (antenna), AB (abdomen), and LE (leg). The *HvGST* expression levels in different adult tissues were normalized relative to those in the 3-d-old adults. Different letters indicate significant differences at $P < 0.05$ according to one-way analysis of variance (ANOVA), followed by Tukey's test. The data represent the mean ± SD of three biological replicates.

insects (Fig. 5). Moreover, exposure to beta-cypermethrin led to significantly lower mRNA levels of *HvGSTd2*, *HvGSTe3*, *HvGSTo1*, and *HvGSTu2* than that in the control insects (Fig. 5).

Discussion

In recent years, several transcriptome data sets have been efficiently applied to search the *GST* genes for nonmodel species with no reference genomic resources, such as *Bradysia odoriphaga* Yang & Zhang (Chen et al. 2015), *Spodoptera litura* Fabricius (Zhang et al. 2016), and *Daktulosphaira vitifoliae* Fitch (Zhao et al. 2018). In the current study, 16 *GST* genes were identified in the adult transcriptome of *H. vitessoides*. The number of *GST* genes identified in *H. vitessoides* was clearly lower than that identified in other lepidopteran species, such as *B. mori*, which has 24 *GST* genes (Yu et al. 2008). This might be explained in two ways; first, previous studies investigated the expression of *GST* genes in all developmental stages, and the expression of several *GST* genes might only be induced by xenobiotics (Enayati et al. 2005, Liao et al. 2013). In contrast, we only searched the *GST* genes in the adult transcriptome of *H. vitessoides*, and might have missed *GST* genes from other developmental stages, as well as xenobiotics-induced *GST* genes; and second, the current sequencing technology might not be sufficiently powerful to screen all genes, especially the transcripts expressed at very low levels (Sheng et al. 2017).

Many studies have reported that several lepidopteran GST genes are abundantly expressed in the midgut, Malpighian tubules, and fat body, which are important metabolic detoxification tissues of insects, are capable of degrading endobiotic and xenobiotic compounds and protecting cells from oxidative damage (Dow and Davies 2006, Arrese and Soulages 2010, Hakim et al. 2010). Our results, obtained with *H. vitessoides*, indicated that the 16 *HvGST* genes were predominately expressed in all or at least one of the tested tissues. The high-level expression of the *HvGST* genes in these tissues suggested their potential roles in physiological metabolism and the detoxification of xenobiotics, such as plant secondary metabolites.

In various adult tissues of *H. vitessoides*, we found that the expression levels of most *HvGST* genes in the abdomen were significantly higher than those in the other adult tissues. Similar results were obtained in *Cnaphalocrocis medinalis* Guenée and *Chilo suppressalis* Walker (Liu et al. 2015a,b). In addition, insect GSTs, such as *BmGSTD4* in *B. mori* (Tan et al. 2014) and *GST-msolf1* in *Manduca sexta* Linnaeus (Rogers et al. 1999), function as odorant-degrading enzymes, which are specifically expressed in the antennae and play an important role in mediating the olfactory signal inactivation that protects the olfactory receptor neurons (Leal 2013). In addition, several insect GSTs, such as *CmGSTd1* in *C. medinalis* (Liu et al. 2015b), *CsupGSTd1* in *C. suppressalis* (Liu et al. 2015b), *BmGSTd1*, *BmGSTd2*, and *BmGSTe1* in *B. mori* (Yu et al. 2008), have been found to be ubiquitously expressed in the antennae and other adult tissues, and are listed as candidate genes of odorant-degrading enzymes. Similarly, in the present study, we found that *HvGSTd1*, which was primarily detected in the abdomen and antennae, might be important both in the degradation of odorants and in the detoxification of xenobiotics. However, further study is necessary to provide an in-depth confirmation of the above hypothesis.

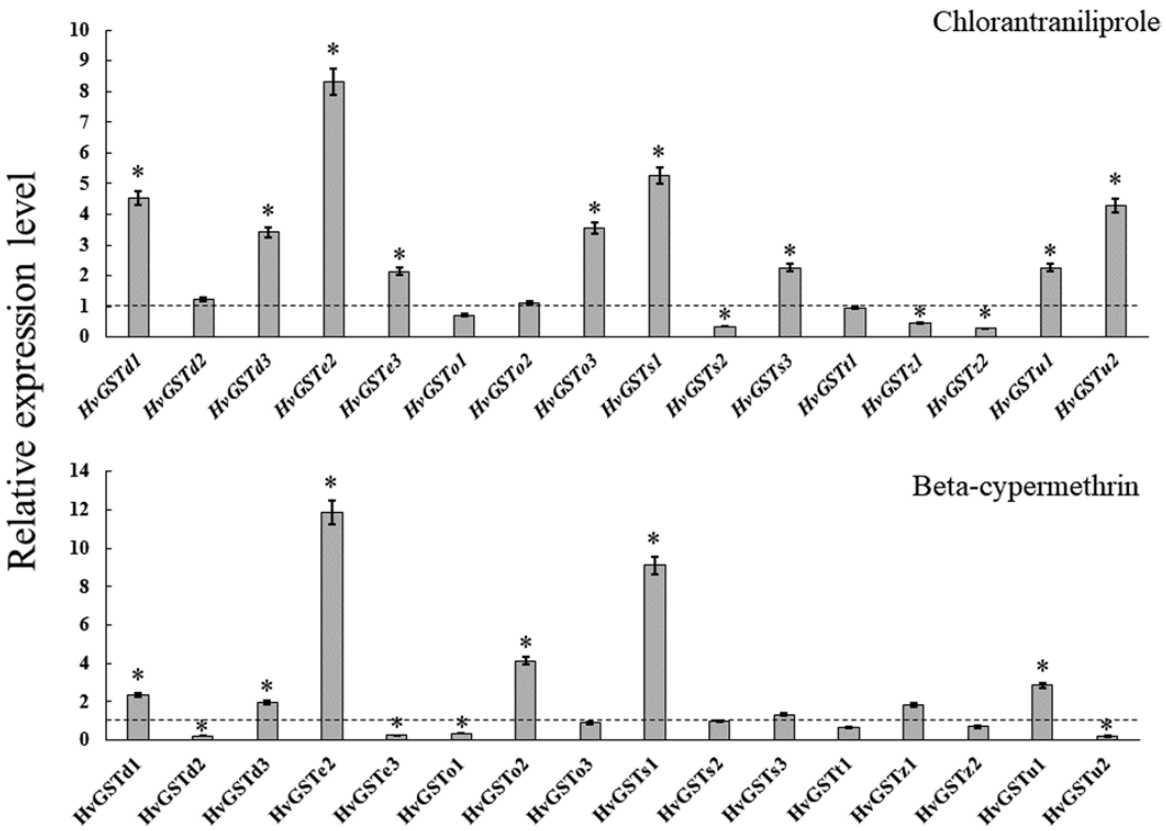

Fig. 5. Relative expression levels of 16 *HvGST* genes in the fourth-instar larvae exposed to the half lethal concentrations (LC_{50}s) of chlorantraniliprole and beta-cypermethrin. The dashed line represents the normalized level of gene expression in the control larvae. The asterisk (*) indicates a significant difference in transcription levels between the treated and control insects (paired Student's *t*-test, $P < 0.05$). The data represent the mean ± SD of three biological replicates.

As mentioned above, conventional insecticides are currently essential for the control of *H. vitessoides*; however, it has become difficult to effectively control this pest with these insecticides. An important mechanism that gives rise to insecticide tolerance is the metabolism of insecticides by the overexpressed GST genes (Han et al. 2016). Accordingly, the identification of insecticide-inducible GSTs might lead to the identification of candidate genes that are connected with insecticide tolerance. Several studies indicate that different insect GST classes participate in the detoxification of chlorantraniliprole and beta-cypermethrin. For example, the expression of nine genes (*PrGSTd1*, *PrGSTd2*, *PrGSTe1*, *PrGSTe2*, *PrGSTe3*, *PrGSTs1*, *PrGSTs3*, *PrGSTs4*, and *PrGSTz1*) was significantly upregulated by a sublethal dose of chlorantraniliprole, and a sublethal dose of lambda-cyhalothrin also significantly elevated the expression of 10 genes (*PrGSTd1*, *PrGSTd3*, *PrGSTe1*, *PrGSTe2*, *PrGSTo1*, *PrGSTo2*, *PrGSTs1*, *PrGSTs2*, *PrGSTs3*, and *PrGSTz2*) in *Pieris rapae* Linnaeus (Liu et al. 2017). Furthermore, in *Plutella xylostella* Linnaeus (Chen and Zhang 2015), four GSTs (*PxGSTd3*, *PxGSTd4*, *PxGSTo2*, and *PxGSTz1*) were found to be significantly overexpressed after exposure to the LC_{10} of beta-cypermethrin. In this study, five *HvGST* genes (*HvGSTd1*, *HvGSTd3*, *HvGSTe2*, *HvGSTs1*, and *HvGSTu1*) were significantly upregulated following exposure to the LC_{50}s of chlorantraniliprole and beta-cypermethrin. Moreover, *HvGSTe3*, *HvGSTo3*, *HvGSTs3*, and *HvGSTu2* were significantly upregulated under the stress of chlorantraniliprole, whereas *HvGSTo2* was upregulated more in the beta-cypermethrin-treated larvae than in the control insects. These genes are therefore potential candidate to be involved in the detoxification of chlorantraniliprole and beta-cypermethrin; however, their expression levels were different, implying that these genes likely play different roles in resistance to chlorantraniliprole and beta-cypermethrin. RNA interference (RNAi) is a universal gene-silencing technology and has been successfully used to investigate the function of GSTs in many insect species. For example, in *Locusta migratoria* Linnaeus, the nymph mortalities increased by 28 and 12% after *LmGSTs5* and *LmGSTu1*, respectively, were silenced by carbaryl treatment (Qin et al. 2013). Additionally, the RNAi-mediated silencing of two *Nilaparvata lugens* Stål GST genes, *NlGSTe1* and *NlGSTm2*, significantly increased the sensitivity of nymphs to chlorpyrifos (Zhou et al. 2013). By using the RNAi approach, further investigations on the function of these potential candidate genes involved in the detoxification of insecticides will help in the elucidation of the mechanism of *H. vitessoides* tolerance to insecticides and provide new strategies for its effective control.

On the contrary, we found that the expression of three (*HvGSTs2*, *HvGSTz1*, and *HvGSTz2*) and four (*HvGSTd2*, *HvGSTe3*, *HvGSTo1*, and *HvGSTu2*) *HvGST* genes were significantly downregulated by chlorantraniliprole and beta-cypermethrin, respectively. The downregulation of GST genes by various insecticides has been reported in several insect species. In *C. medinalis* (Liu et al. 2015a), for example, the expression of five GST genes, *CmGSTe1*, *CmGSTe4*, *CmGSTe5*, *CmGSTz1*, and *CmGSTu1*, was downregulated by chlorpyrifos exposure. Similarly, an exposure to cyhalothrin, fipronil, or endosulfan reduced the expression levels of two GST genes (*LdGSTe4* and *LdGSTe6*) in *Leptinotarsa decemlineata* Say (Han et al. 2016). This phenomenon was considered an adaptive homeostasis and

an energy trade-off strategy, wherein the energy was focused to express the most crucial detoxification genes when the insects exposed to insecticides (Jing et al. 2017).

The expression levels of the remaining four *HvGST genes* (*HvGSTd2*, *HvGSTo1*, *HvGSTo2*, and *HvGSTt1*) and six *HvGST* genes (*HvGSTo3*, *HvGSTs2*, *HvGSTs3*, *HvGSTt1*, *HvGSTz1*, and *HvGST2*) showed no significant changes after exposure to chlorantraniliprole and beta-cypermethrin, respectively. These results indicated that these GSTs might be related to the detoxification of other insecticides that were not tested in this study, or that these genes were not sufficiently activated after a 24-h exposure period.

In summary, we identified 16 full-length cytosolic GST sequences from the adult transcriptome of *H. vitessoides*. The spatial analysis of expression patterns showed that the 16 *HvGST* genes exhibited distinct expression levels in different larval and adult tissues. After chlorantraniliprole and beta-cypermethrin exposures, the expression of several *HvGST* genes, which are the potential candidates involved in the detoxification of these insecticides, was significantly upregulated.

Supplementary Data

Supplementary data are available at *Journal of Insect Science* online.

Acknowledgments

This work was supported by grants from the National Natural Science Foundation of China (31470653) and the Natural Science Foundation of Guangdong Province, China (2015A030313416).

References Cited

Arrese, E. L., and J. L. Soulages. 2010. Insect fat body: energy, metabolism, and regulation. Annu. Rev. Entomol. 55: 207–225.

Chen, X. E., and Y. L. Zhang. 2015. Identification and characterisation of multiple glutathione S-transferase genes from the diamondback moth, *Plutella xylostella*. Pest Manag. Sci. 71: 592–600.

Chen, Z. Y., L. F. Zheng, L. Wang, D. W. Li, C. L. Cao, and Y. Z. Li. 2011. Studies on the synergistic effects of chlorantraniliprole and beta-cypermethrin on *Heortia vitessoides* Moore. J. Shandong For. Sci. Technol. 6: 48–49.

Chen, H. L., L. L. Lin, M. H. Xie, G. L. Zhang, and W. H. Su. 2015. *De novo* sequencing and characterization of the *Bradysia odoriphaga* (Diptera: Sciaridae) larval transcriptome. Comp. Biochem. Physiol. Part D Genomics Proteomics. 16: 20–27.

Cheng, J., J. X. Chen, and T. Lin. 2017. *De novo* assembly and analysis of the *Heortia vitessoides* transcriptome via high-throughput Illumina sequencing. J. Asia Pac. Entomol. 20: 1241–1248.

Cheng, J., Z. H. Lyu, and T. Lin. 2018. Identification and expression analysis of thioredoxin peroxidase gene in *Heortia vitessoides*. J. Huazhong Agric. Univ. 37: 56–63.

Dow, J. A. T., and S. A. Davies. 2006. The Malpighian tubule: rapid insights from post-genomic biology. J. Insect Physiol. 52: 365–378.

Enya, S., T. Daimon, F. Igarashi, H. Kataoka, M. Uchibori, H. Sezutsu, T. Shinoda, and R. Niwa. 2015. The silkworm glutathione S-transferase gene noppera-bo is required for ecdysteroid biosynthesis and larval development. Insect Biochem. Mol. Biol. 61: 1–7.

Enayati, A. A., H. Ranson, and J. Hemingway. 2005. Insect glutathione transferases and insecticide resistance. Insect Mol. Biol. 14: 3–8.

Feng, Q. L., K. G. Davey, A. S. Pang, M. Primavera, T. R. Ladd, S. C. Zheng, S. S. Sohi, A. Retnakaran, and S. R. Palli. 1999. Glutathione S-transferase from the spruce budworm, *Choristoneura fumiferana*: identification, characterization, localization, cDNA cloning, and expression. Insect Biochem. Mol. Biol. 29: 779–793.

Hakim, R. S., K. Baldwin, and G. Smagghe. 2010. Regulation of midgut growth, development, and metamorphosis. Annu. Rev. Entomol. 55: 593–608.

Han, J. B., G. Q. Li, P. J. Wan, T. T. Zhu, and Q. W. Meng. 2016. Identification of glutathione S-transferase genes in *Leptinotarsa decemlineata* and their expression patterns under stress of three insecticides. Pestic. Biochem. Physiol. 133: 26–34.

Huang, Y. F., Z. B. Xu, X. Y. Lin, Q. L. Feng, and S. C. Zheng. 2011. Structure and expression of glutathione S-transferase genes from the midgut of the common cutworm, *Spodoptera litura* (Noctuidae) and their response to xenobiotic compounds and bacteria. J. Insect Physiol. 57: 1033–1044.

Huang, X. L., D. S. Fan, L. Liu, and J. N. Feng. 2017. Identification and characterization of glutathione S-transferase genes in the antennae of codling moth (Lepidoptera: Tortricidae). Ann. Entomol. Soc. Am. 110: 409–416.

Jin, X. F., T. Ma, M. S. Chang, Y. J. Wu, Z. T. Liu, Z. H. Sun, T. J. Shan, X. Y. Chen, X. J. Wen, and C. Wang. 2016. Aggregation and feeding preference of gregarious *Heortia vitessoides* (Lepidoptera: Crambidae) larvae to *Aquilaria sinensis* (Thymelaeaceae). J. Entomol. Sci. 51: 209–218.

Jing, T. X., Y. X. Wu, T. Li, D. D. Wei, G. Smagghe, and J. J. Wang. 2017. Identification and expression profiles of fifteen delta-class glutathione S-transferase genes from a stored-product pest, *Liposcelis entomophila* (Enderlein) (Psocoptera: Liposcelididae). Comp. Biochem. Physiol. B Biochem. Mol. Biol. 206: 35–41.

Kalita, J., P. R. Bhattacharyya, and S. C. Nath. 2002. *Heortia vitessoides* Moore (Lepidoptera: Pyralidae): a serious pest of agarwood plant (*Aquilaria malaccensis* Lamk.). Geobios. 29: 13–16.

Labade, C. P., A. R. Jadhav, M. Ahire, S. S. Zinjarde, and V. A. Tamhane. 2018. Role of induced glutathione-S-transferase from *Helicoverpa armigera* (Lepidoptera: Noctuidae) HaGST 8 in detoxification of pesticides. Ecotoxicol. Environ. Saf. 147: 612–621.

Leal, W. S. 2013. Odorant reception in insects: roles of receptors, binding proteins, and degrading enzymes. Annu. Rev. Entomol. 58: 373–391.

Liao, C. Y., K. Zhang, J. Z. Niu, T. B. Ding, R. Zhong, W. K. Xia, W. Dou, and J. J. Wang. 2013. Identification and characterization of seven glutathione S-transferase genes from citrus red mite, *Panonychus citri* (McGregor). Int. J. Mol. Sci. 14: 24255–24270.

Liu, S., X. J. Rao, M. Y. Li, M. F. Feng, M. Z. He, and S. G. Li. 2015a. Glutathione S-transferase genes in the rice leaffolder, *Cnaphalocrocis medinalis* (Lepidoptera: Pyralidae): identification and expression profiles. Arch. Insect Biochem. Physiol. 90: 1–13.

Liu, S., Z. J. Gong, X. J. Rao, M. Y. Li, and S. G. Li. 2015b. Identification of putative carboxylesterase and glutathione S-transferase genes from the antennae of the *Chilo suppressalis* (Lepidoptera: Pyralidae). J. Insect Sci. 15: 103.

Liu, S., Y. X. Zhang, W. L. Wang, B. X. Zhang, and S. G. Li. 2017. Identification and characterisation of seventeen glutathione S-transferase genes from the cabbage white butterfly *Pieris rapae*. Pestic. Biochem. Physiol. 143: 102–110.

Pfaffl, M. W. 2001. A new mathematical model for relative quantification in real-time RT-PCR. Nucleic Acids Res. 29: 2002–2007.

Qiao, H. L., P. F. Lu, J. Chen, W. S. Ma, R. M. Qin, and X. M. Li. 2012. Antennal and behavioural responses of *Heortia vitessoides* females to host plant volatiles of *Aquilaria sinensis*. Entomol. Exp. Appl. 143: 269–279.

Qiao, H. L., P. F. Lu, J. Chen, C. Q. Xu, W. S. Ma, R. M. Qin, X. M. Li, and H. Z. Cheng. 2013. Biological characteristics and occurrence patterns of *Heortia vitessoides*. Chin. J. Appl. Entomol. 50: 1244–1252.

Qin, G. H., J. Miao, T. Liu, X. Y. Zhang, Y. P. Guo, K. Y. Zhu, E. B. Ma, and J. Z. Zhang. 2013. Characterization and functional analysis of four glutathione *S*-transferases from the migratory locust, *Locusta migratoria*. PLoS One. 8: e58410.

Rogers, M. E., M. K. Jani, and R. G. Vogt. 1999. An olfactory-specific glutathione-S-transferase in the sphinx moth *Manduca sexta*. J. Exp. Biol. 202: 1625–1637.

Sheehan, D., G. Meade, V. M. Foley, and C. A. Dowd. 2001. Structure, function and evolution of glutathione transferases: implications for classification of non-mammalian members of an ancient enzyme superfamily. Biochem. J. 360: 1–16.

Sheng, S., C. W. Liao, Y. Zheng, Y. Zhou, Y. Xu, W. M. Song, P. He, J. Zhang, and F. A. Wu. 2017. Candidate chemosensory genes identified in the endoparasitoid *Meteorus pulchricornis* (Hymenoptera: Braconidae) by antennal transcriptome analysis. Comp. Biochem. Physiol. Part D Genomics Proteomics. 22: 20–31.

Su, Y. P. 1994. The biological characteristic of *Heortia vitessoides*. J. Chin. Med. Mater. 17: 7–9.

Tamura, K., D. Peterson, N. Peterson, G. Stecher, M. Nei, and S. Kumar. 2011. MEGA5: molecular evolutionary genetics analysis using maximum likelihood, evolutionary distance, and maximum parsimony methods. Mol. Biol. Evol. 28: 2731–2739.

Tan, X., X. M. Hu, X. W. Zhong, Q. M. Chen, Q. Y. Xia, and P. Zhao. 2014. Antenna-specific glutathione S-transferase in male silkmoth *Bombyx mori*. Int. J. Mol. Sci. 15: 7429–7443.

Wan, H., S. Zhan, X. Xia, P. Xu, H. You, B. R. Jin, and J. Li. 2016. Identification and functional characterization of an epsilon glutathione S-transferase from the beet armyworm (*Spodoptera exigua*). Pestic. Biochem. Physiol. 132: 81–88.

Yamamoto, K., and N. Yamada. 2016. Identification of a diazinon-metabolizing glutathione S-transferase in the silkworm, *Bombyx mori*. Sci. Rep. 6: 30073.

Yu, Q., C. Lu, B. Li, S. Fang, W. Zuo, F. Dai, Z. Zhang, and Z. Xiang. 2008. Identification, genomic organization and expression pattern of glutathione S-transferase in the silkworm, *Bombyx mori*. Insect Biochem. Mol. Biol. 38: 1158–1164.

Zhang, X. Y., J. X. Wang, M. Zhang, G. H. Qin, D. Q. Li, K. Y. Zhu, E. B. Ma, and J. Z. Zhang. 2014. Molecular cloning, characterization and positively selected sites of the glutathione S-transferase family from *Locusta migratoria*. PLoS One. 9: e114776.

Zhang, N., J. Liu, S. N. Chen, L. H. Huang, Q. L. Feng, and S. C. Zheng. 2016. Expression profiles of glutathione S-transferase superfamily in *Spodoptera litura* tolerated to sublethal doses of chlorpyrifos. Insect Sci. 23: 675–687.

Zhao, J. J., D. S. Fan, Y. Zhang, and J. N. Feng. 2018. Identification and characterisation of putative glutathione S-transferase genes from *Daktulosphaira vitifoliae* (Hemiptera: Phylloxeridae). Environ. Entomol. 47: 196–203.

Zhou, W. W., Q. M. Liang, Y. Xu, G. M. Gurr, Y. Y. Bao, X. P. Zhou, C. X. Zhang, J. Cheng, and Z. R. Zhu. 2013. Genomic insights into the glutathione S-transferase gene family of two rice planthoppers, *Nilaparvata lugens* (Stål) and *Sogatella furcifera* (Horváth) (Hemiptera: Delphacidae). PLoS One. 8: e56604.